BBC RD 1974/31

BBC

RESEARCH DEPARTMENT

1969 1974
THE QUEEN'S AWARD TO INDUSTRY

REPORT

AG

Laser beam deflection

I. Childs, B.A., Ph.D.

Research Department, Engineering Division
THE BRITISH BROADCASTING CORPORATION September 1974

BBC RD 1974/31
UDC 621.375.9.

LASER BEAM DEFLECTION

I. Childs, B.A., Ph.D.

Summary

In the first part of this report, the design of a prototype laser deflection system is described, together with some of the principles behind the deflection method chosen. The measured performance of the system is quoted and methods for improving this performance outlined. In the second part, a comparison is made between the various methods of laser deflection and some comments made as to the suitability of these methods to broadcasting applications that are at present envisaged.

Issued under the authority of

P. Lange

Head of Research Department

Research Department, Engineering Division,
BRITISH BROADCASTING CORPORATION

September 1974

(PH-132)

LASER BEAM DEFLECTION

LASER BEAM DEFLECTION

I. Childs, B.A., Ph.D.

Part I

1. Introduction

This Report is concerned with deflection and scanning of light beams. There are two main areas in which the application of such techniques to broadcasting have been envisaged. The first is the production of a scanned raster for use in a telecine-machine, slide-scanner or television projection display system; at present, these use cathode-ray tubes and suffer, in the first two cases, from problems of afterglow and, in the third case, from rather inadequate light output. A light-beam scanning system could eliminate these problems. It should be noted, however, that coherent light sources are not absolutely necessary for these uses, although they would enable smaller spot sizes to be achieved.

The other main proposed area of application, which does demand coherent light, is the 'read-out' of a digital holographic store; such a system is at present being considered. A series of holograms is exposed on one frame of a 16 or 35 mm film, each hologram representing a multiple-bit digital word. On replay, the laser beam scans each hologram sequentially in order to recover the recorded data pattern.

For the first area of application, the light output should contain components at wavelengths corresponding to red, green and blue. The three components should be well registered at all deflections and their intensities should not vary unduly with the deflection. The application to holographic read-out, however, requires only one colour, and, because it is only necessary to recognise the presence or absence of light at points in the reconstructed pattern, the intensity need not be closely controlled. The scanning requirements are also different; the first application requires a linear sawtooth scan while for the second, a 'stepping' action is preferred.

Many methods exist, in principle, for performing either operation and a survey is given later in Part 2 of this Report. It was decided to investigate more thoroughly one of the more promising deflection techniques – that employing an acousto-optic grating – and, to that end, a simple deflection cell was obtained. In the following section, a description of this deflection technique is given.

2. The acousto-optic grating

The method of operation of this device is illustrated in Fig. 1. A periodic sound wave passing through a suitable medium, which may be gaseous, liquid or a solid crystal, set up a periodic variation in refractive index. A light beam passing simultaneously through the cell interacts with this periodic structure and is scattered into a regular pattern similar to that encountered in a diffraction grating. The 'pitch' of this diffraction pattern, i.e. the deflection

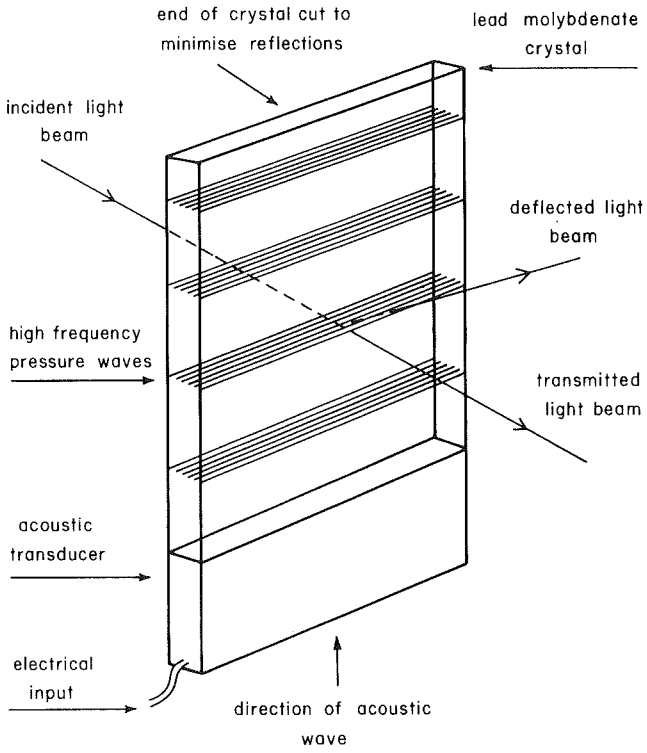

Fig. 1 - Principle of the acousto-optic light deflector

produced by the acoustic cell, is proportional to the frequency of the sound wave. Likewise the intensity of the diffracted light is a function of the power in the sound wave, all undiffracted light passing straight through the cell and forming an undeflected beam.

If the medium has negligible thickness (compared with the wavelength of the sound wave) the familiar Raman-Nath[1] diffraction pattern appears with the light splitting into many orders. However, if the interaction length in the medium is large (the condition usually quoted[2] is $\lambda l/2\Lambda > \pi$, where λ is the wavelength of the incident light beam in air, Λ the wavelength of the sound wave in the diffraction medium and l the thickness of the medium) then a situation analogous to the Bragg diffraction emchanism in X-ray crystallography occurs with the light passing mainly into one order. It is this diffraction mechanism which is usually produced because, in most cases, the presence of other orders is undesirable. It is worth noting that Brillouin first predicted this acousto-optic diffraction in 1921[3] but it was not until 1932 that the effect was experimentally produced.[4]

Referring to Fig. 2a it may be seen that the diffracted waves will reinforce if the path-difference is an integral number of optical wavelengths, i.e. if

$$B'C' + D'E' = m\lambda \quad (1)$$

This occurs when:

$$\Lambda \sin\theta_1 + \Lambda \sin\theta_2 = m\lambda \quad (2)$$

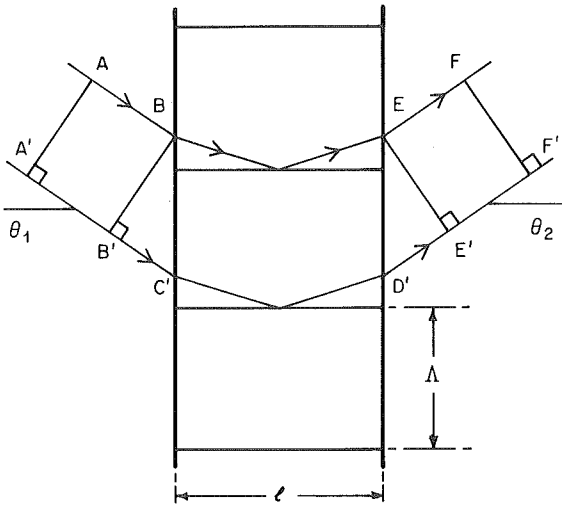

(a)

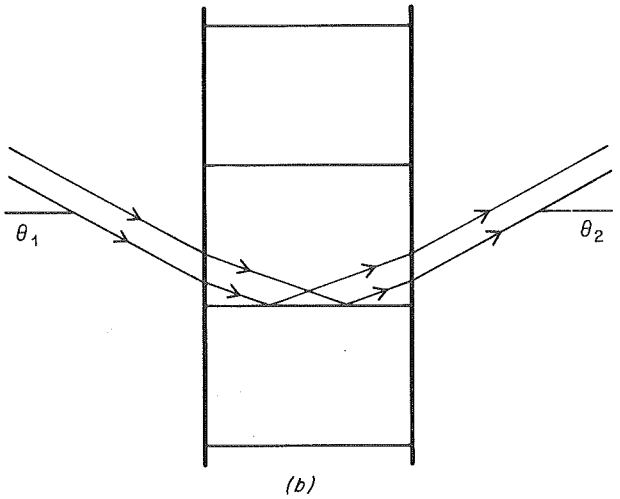

(b)

Fig. 2 - Path of light rays through the deflector

In addition, the diffractions produced from the same acoustic wavefront will also re-inforce (see Fig. 2b) when $\theta_1 = \theta_2$. It is this re-inforcing that produces the Bragg effect. For other angles of deflection, not all the light beams re-inforce although there may be sufficient re-inforcement to produce a very dim beam. As the thickness of the diffraction medium increases, so the intensity of these unwanted orders decreases. A full mathematical treatment is given by Gordon[5] and a summary of the literature by Quate et al.[6]

A practical deflection cell requires that the acoustic frequency be altered in order to change the total deflection of the beam. From equation (2) assuming $m = 1$, and small angles θ_1, θ_2:

$$\sin\theta_1 + \sin\theta_2 \doteq \theta_1 + \theta_2 = \theta_d = \frac{\lambda}{\Lambda} = \frac{\lambda}{V} f \quad (3)$$

where f is the acoustic frequency and V is the acoustic velocity in the diffraction medium, from now on assumed to be a solid crystal. If f is varied over its maximum range, Δf, the maximum change in deflection angle of the beam, $\Delta\theta_d$, is therefore

$$\Delta\theta_d = \frac{\lambda}{V} \cdot \Delta f \quad (4)$$

Owing to diffraction, the minimum size of a focussed spot is determined by the effective diameter of the deflected beam.

Assuming spatial coherence at the input, the first nulls of the far-field pattern will be at angles of $\pm \pi/D$ to the central maximum, where D is the effective aperture of the beam, usually governed by the dimensions of the crystal. Following convention, π/D is defined as the smallest resolvable angle θmin. Therefore the number of resolvable spots in the scan, N is:

$$N = \frac{\Delta\theta d}{\theta \min} = \frac{D}{kV} \cdot \Delta f = \frac{\tau \cdot \Delta f}{k} \quad (5)$$

(where k is a factor to allow for the beam shape: $k = 1{\cdot}22$ for a uniform circular beam).

where τ is the transit time of the sound wave across the aperture D.

Thus, for high resolution, τ should be large. But the transit time should not be larger than the time interval within which it is desired to switch the beam from one position to the next, although in the special case of a linear sawtooth scan where there is a constant rate of change of frequency across the optical aperture, the defects caused by exceeding this limit may be corrected by a cylindrical lens.[7,8]

In addition to the limit on τ, there is also a limit on Δf, set by the thickness of the cell. As has been noted, the maximum intensity of the deflected beam occurs at the Bragg angle of incidence. At other acoustic frequencies the angle of incidence will not be correct and light loss will result. The usual value quoted for this 'angular tolerance limit'[7] is $\pm$ ½ Λ/l radians, corres-

ponding to a light loss of $4/\pi^2$, or about 4 dB (l has been defined as the thickness of the crystal). Korpel et al[7] have shown that it is possible to tilt the acoustic wavefront so that, to a first order approximation, the Bragg angle is tracked by the incident light beam and the tolerance limit is increased. They also show that the efficiency of the cell (i.e. the proportion of the incident light that is diverted into the deflected beam) is related to the input power by an equation of the form

$$\eta = \sin^2 A\sqrt{Pl} \qquad (6)$$

where η is the efficiency, P the input acoustic power and A is a constant. Thus it is theoretically possible to operate the device at 100% efficienty and at this input power level, the efficiency is only slightly affected by variations in the acoustic power over the input frequency range, Δf.

The deflection cell used in the prototype was a lead molybdate deflector. If had a nominal input impedance (to the acoustic transducer) of 50 Ω over a bandwidth of 55MHz centred on 110MHz. The time-bandwidth product, $\tau\ \Delta f$ was 106 indicating a resolution of approximately 80 spots. (k is usually between 1·22 and 1·4 for a beam of truncated Gaussian cross-section.) Unfortunately the power rating of the cell was not sufficient to allow operation at the peak of the efficiency curve, being limited to 2W. Nevertheless, the performance of the cell was sufficient to enable a realistic evaluation of the technique to be carried out and to study some of the problems arising.

3. The driving equipment

In order to operate the cell it must be driven from a source of v.h.f. power controlled over a frequency range of 80 – 140 MHz. This input power to the cell must be capable of being controlled, in order to compensate for variations in brightness of the deflected beam, and must be of the order of 2W in magnitude, to obtain the required intensity. A major section of the project was, therefore, to develop the circuitry required to do this.

A block diagram of the prototype system is shown in Fig. 3 and the circuit diagrams in Figs. 4a and b. The voltage-controlled oscillator produces a carrier at a frequency which can be varied over a wide range. The output frequency is detected by the pulse-counting detector, which produces an output voltage proportional to the oscillator frequency. This voltage is compared with the input voltage (representing the desired deflection angle) and the error voltage is amplified and used to correct the oscillator frequency.

The transfer function of the voltage-controlled oscillator (output frequency vs. input voltage) is shown in Fig. 5, and the transfer function of the whole frequency-control loop is shown in Fig. 6. Measured results indicate that the overall linearity of this characteristic, considered as a percentage deviation from the optimum straight line passing through the measured points in the range 80 – 140 MHz, was better than ± 0·25%. Thus any measured point is never further than 0·25% of 60 MHz, or 150 kHz, from the straight line defining the idealised response of the system. The 3 dB bandwidth of the frequency-control loop was measured as 4 MHz and the rise-time to a small step input was measured as 120 'n' sec (to 90%).

Because the pulse-counting detector is temperature-sensitive, drift characteristics were measured and the results are plotted in Figs. 7a and 7b. Fig. 7a shows the drift immediately after switch-on and it is seen that the frequency stabilises to within 1% (one spot) after 10 minutes and to its final value after ½ hour. When the output frequency suddenly changes from one constant value to another, the mean current through the pulse-counting detector is also changed. Thus the temperature is also affected and the output frequency will show an additional thermal drift. Fig. 7b shows that this is small (about 1% of the initial frequency change) and of a long time-constant. For these reasons it is unlikely to cause any severe problems.

The v.h.f. signal then passes to a preamplifier and a power amplifier which together raise the level to about 1½ W into 50 Ω. In order to compensate for output mismatch, the output power fed to the load, as measured by two directional couplers, is sensed and used to control the gain of the preamplifier. This a.g.c. loop therefore keeps the output power level over the frequency range independent of the output load impedance, within reason-

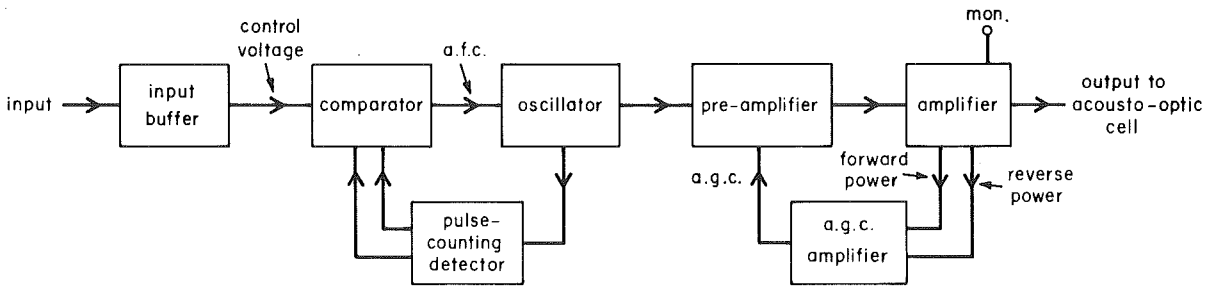

Fig. 3 - Block diagram of the driving circuitry

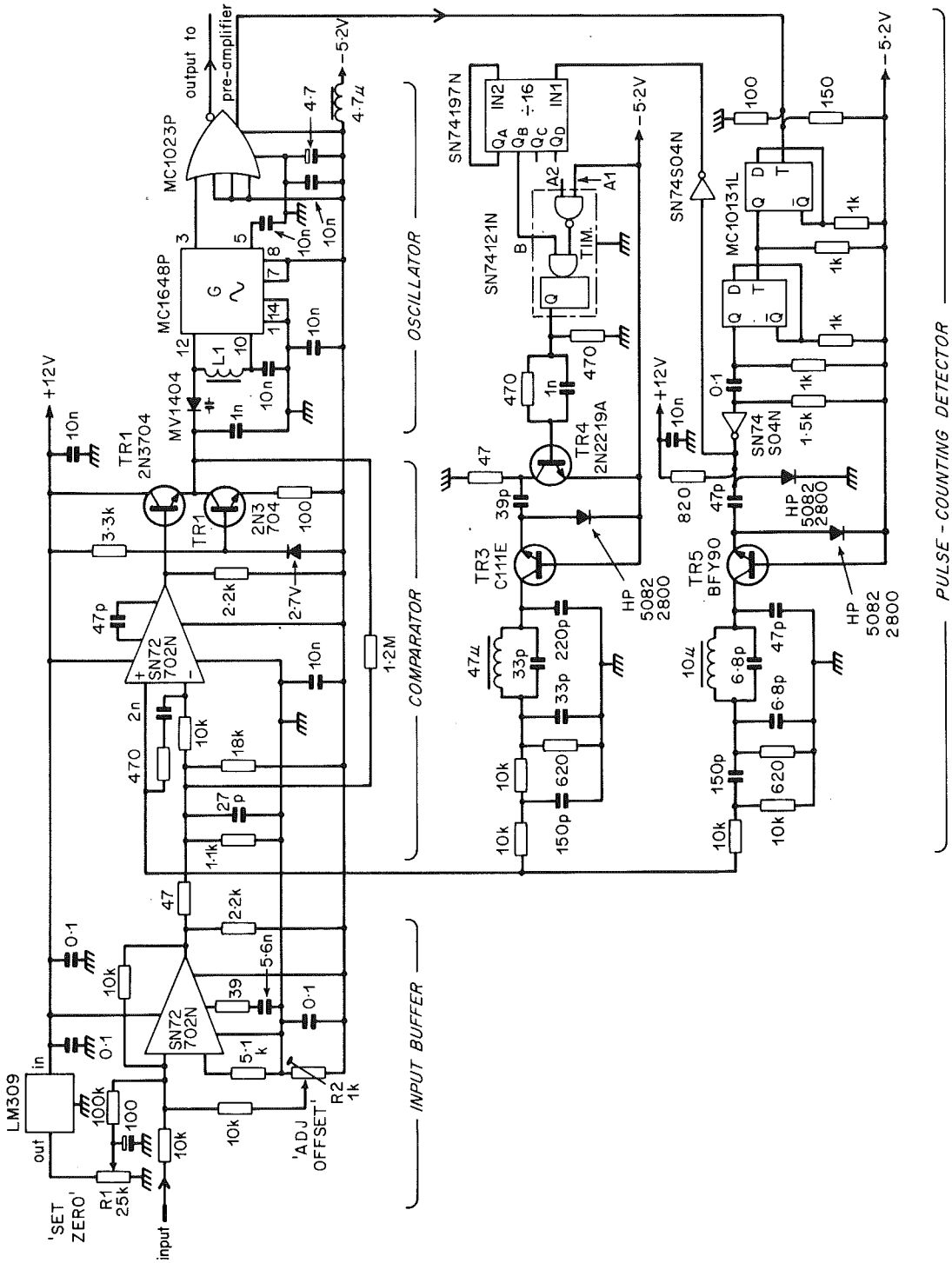

Fig. 4a - Circuit diagram of the driving equipment

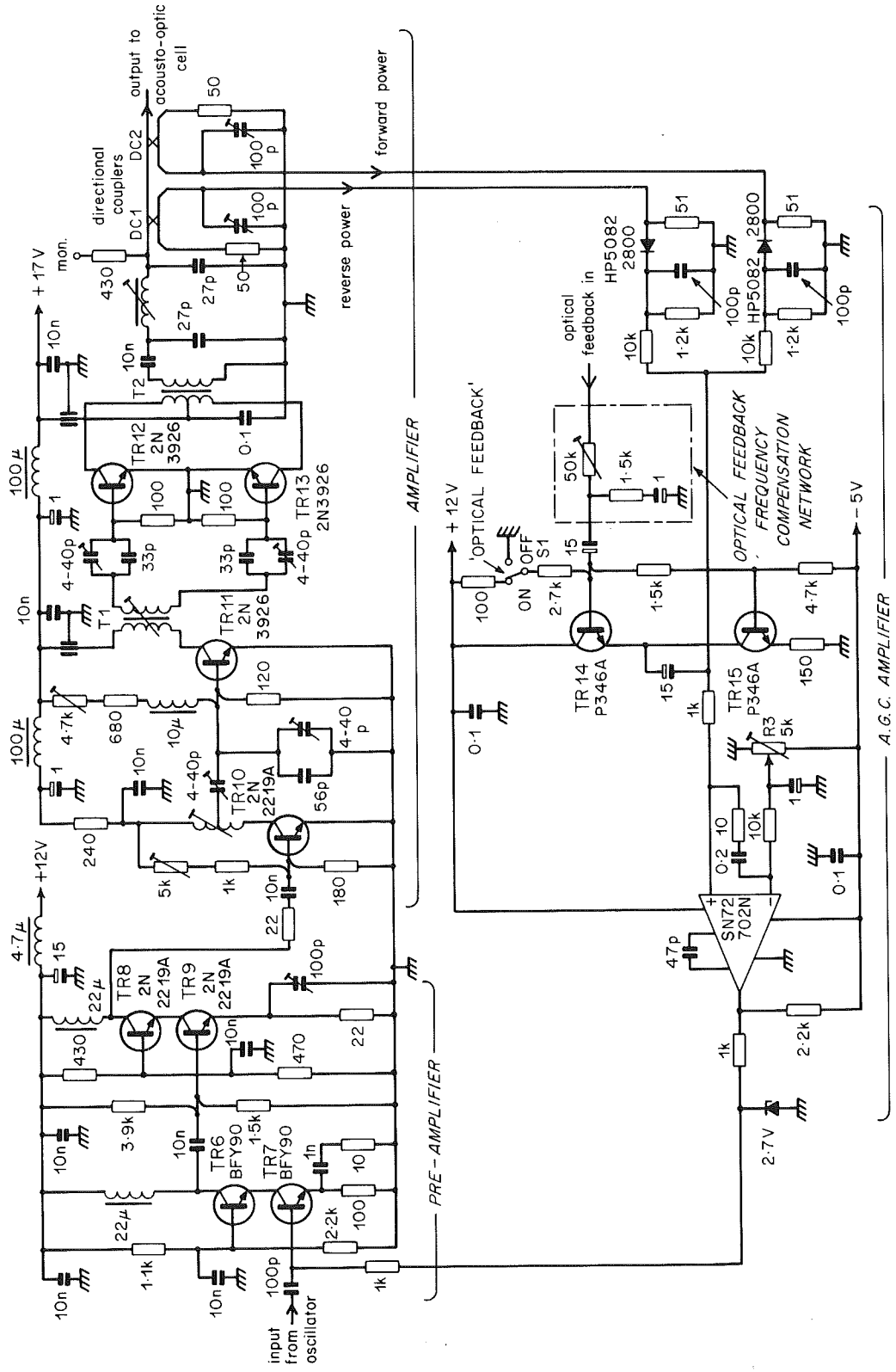

Fig. 4b - Circuit diagram of the driving equipment

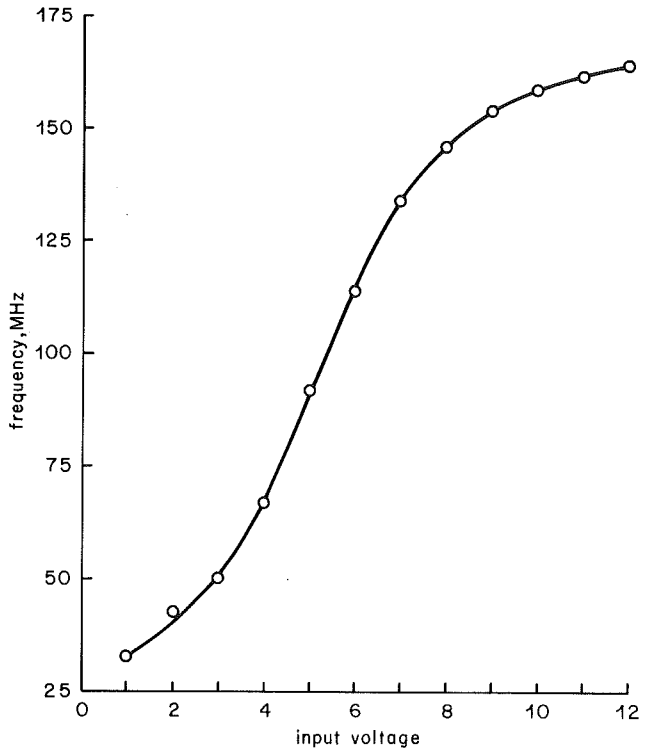

Fig. 5 - Transfer function of the voltage controlled oscillator

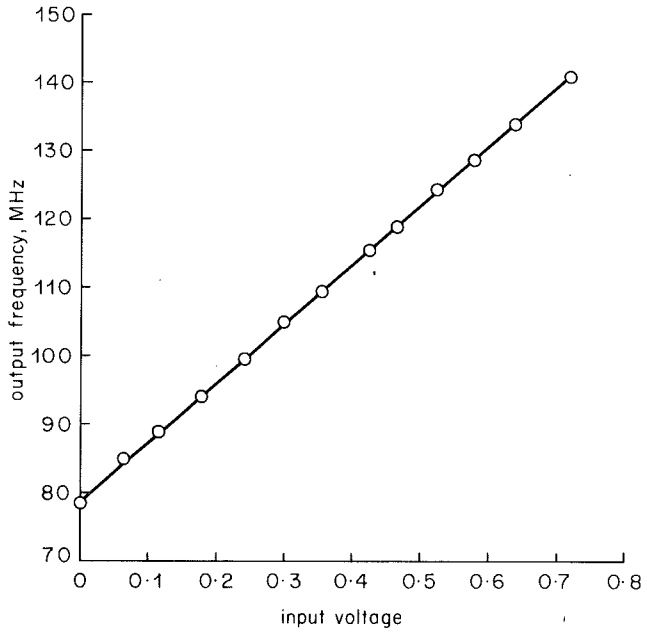

Fig. 6 - Transfer characteristic of the frequency control loop

able limits. Provision is also included for a.c.-coupled feedback from an external photodetector; use of this is described in a later section.

Many of the results quoted in the following sections were taken using a simplified a.g.c. detector which used

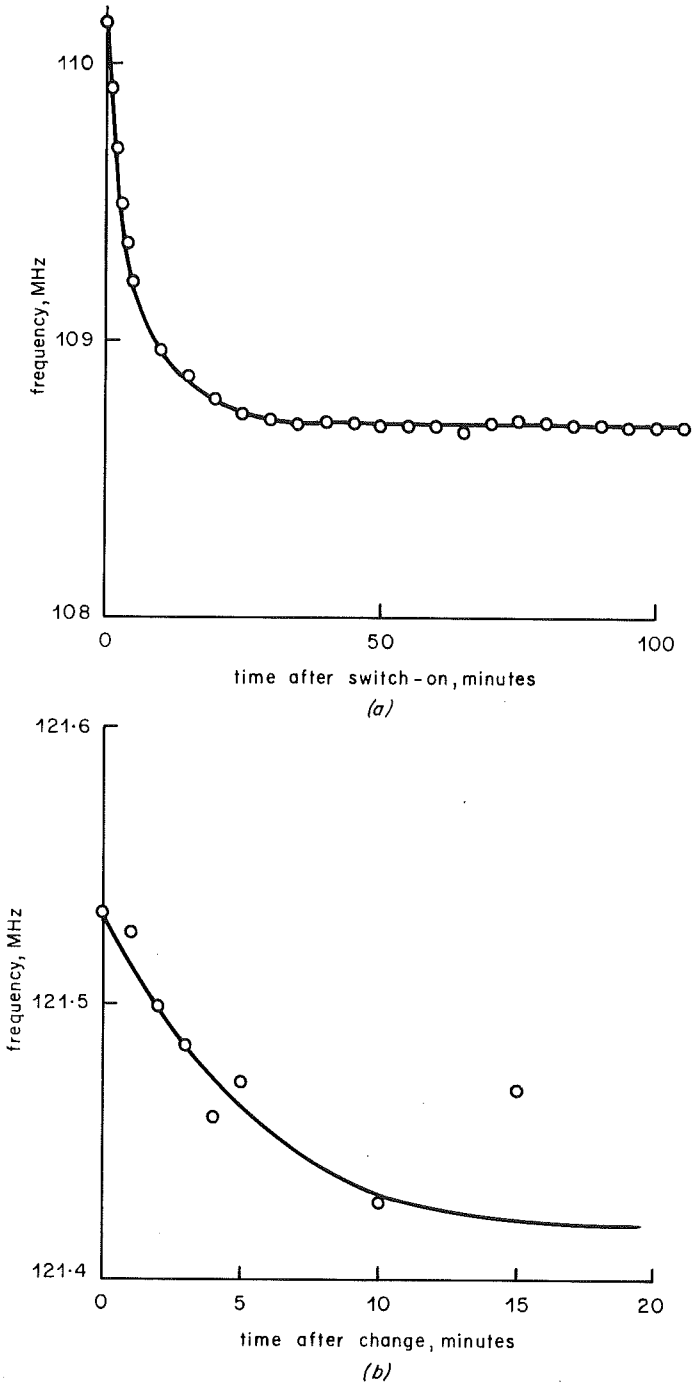

Fig. 7 - Drift of the frequency control loop

(a) after switch on

(b) in response to a sudden change in output frequency

a resistive attenuator in place of the directional couplers. Such a system holds the output voltage constant and not the output power; the effects of this are discussed in a later section, together with the reasons for the choice of the final system.

The performance of the a.g.c. loop was reasonable power being controlled to ±8% for scan frequencies less than 2 kHz, and ±12% for scan frequencies up to 16 kHz. A complete specification of the prototype system appears

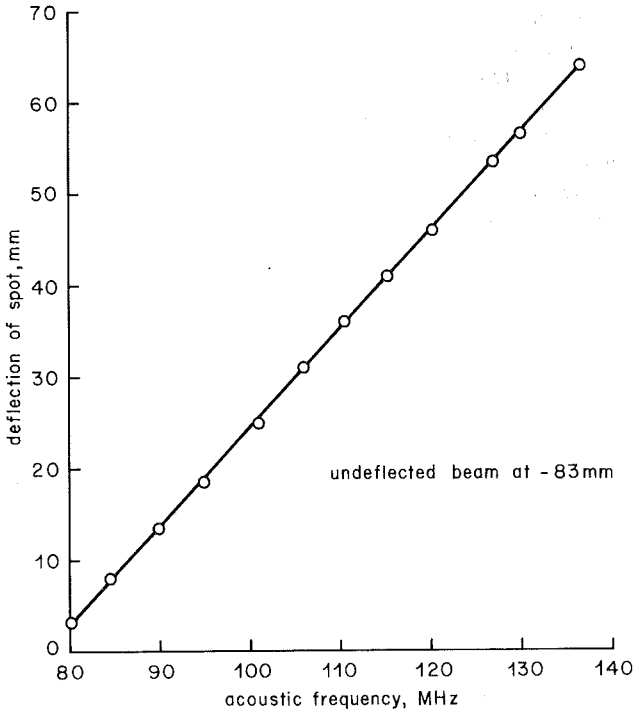

Fig. 8 - Spot deflection vs acoustic frequency

in Appendix 1, and a more detailed description of the individual circuits in Appendix 3.

4. Characteristics of the deflection cell

There are various characteristics that affect the performance of the deflection cell and its suitability for specific applications. The main parameter is the deflection of the spot and the linearity of this deflection as considered against the input frequency. Figure 8 shows the spot deflection for an optical path length of 6·5 m (approx.), plotted against frequency and it is seen that the deviations from linearity are within the bounds of experimental error (~ 1 mm). The total sweep of 61 mm represents an angular scan of approximately 32·3 mins.

Another factor of importance is the variation in the intensity of the deflected spot with position. When it is the acoustic voltage which is held level and not the acoustic power, any mismatch between the acoustic cell and the characteristic impedance of the cable feeding it will cause a varying impedance load to be presented at the output of the main amplifier, and hence a varying power consumption by the acoustic cell. This in turn will cause variation in the intensity of the deflected spot. Fig. 9 shows the intensity of the deflected spot plotted against the acoustic frequency for a constant voltage into the cell and it is seen that the variations are large. Measurements of the input impedance of the cell plus driving cable suggest that the variations are mainly due to the mechanism outlined above.

Because this variation is highly undesirable for a linear scanning application (although it may be tolerable for

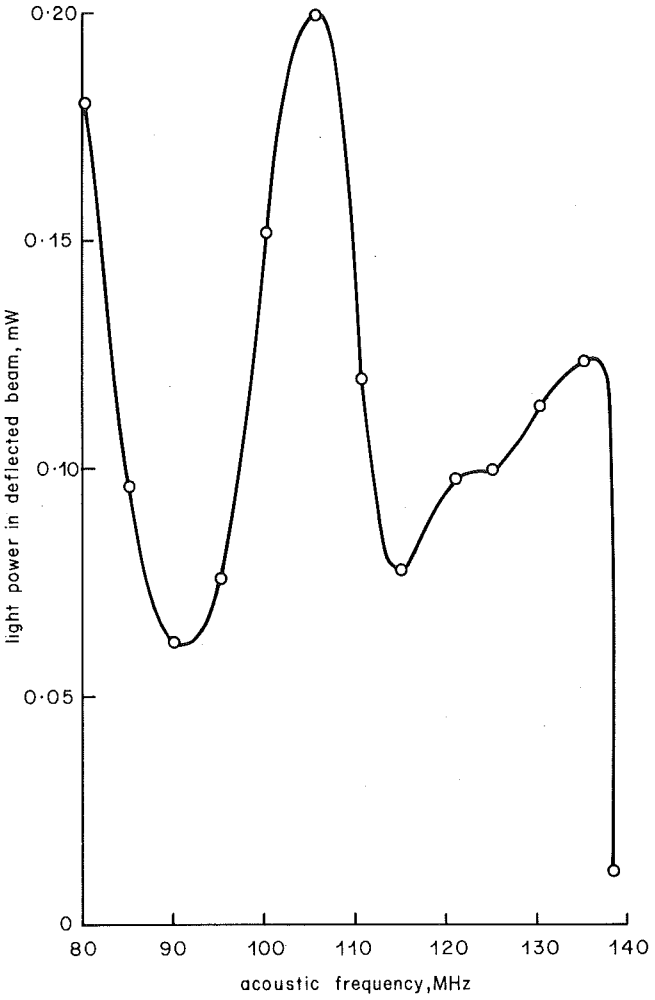

Fig. 9 - Light power in deflected beam vs acoustic frequency

the digital holographic read-out), methods of reducing it were investigated. There are basically three methods. One is to match the impedance of the cell more accurately to the driving impedance.[10] This will always give rise to a residual mis-match, although this can be made to be fairly small by the use of sufficient elements; nevertheless, by itself, this method is probably not sufficient. In addition, experimental results indicate that the impedance of the cell is difficult to equalise effectively. It is possible to make wideband directional couplers with very well controlled characteristics;[11] use of these would enable the a.g.c. signal to be made a function of the power level, not the voltage level. Once again, however, there will be some residual variation. Also the Bragg angle tolerance will introduce a substantial light loss at the band edges. However, this system provides surprisingly good results. Fig. 10 shows the intensity in the deflected beam over a 80—140 MHz scan before and after such a control of power. The intensity variations are reduced substantially. A better method still would be to sense the light intensity in the deflected beam and to provide feedback to hold it constant. This is not always practical, however, so the next best thing must be done; the undeflected beam is held

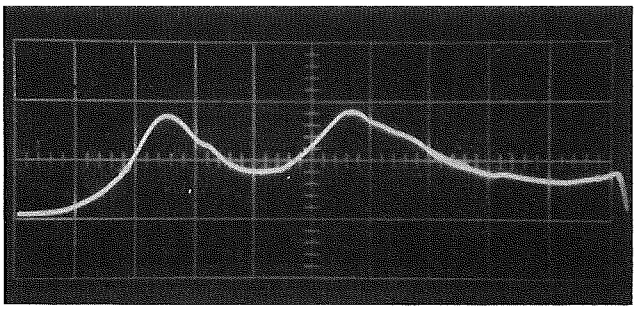

(a)

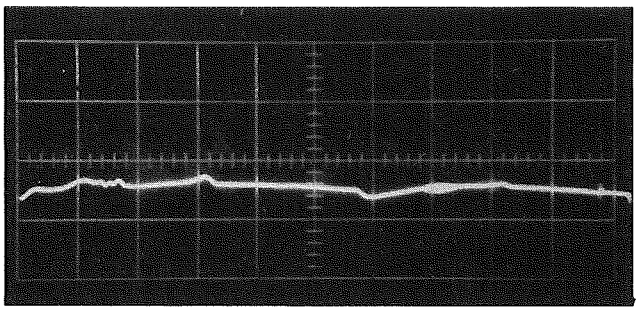

(b)

Fig. 10 - Effect of power levelling
(a) voltage to cell controlled (b) power to cell controlled
Identical Scales

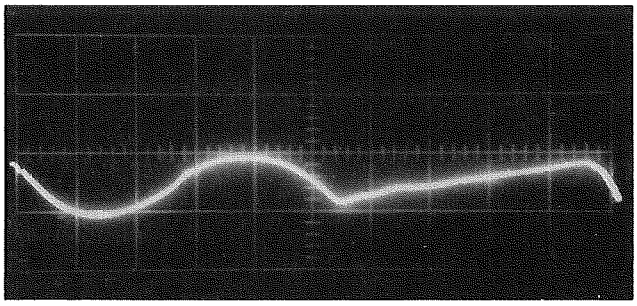

(a)

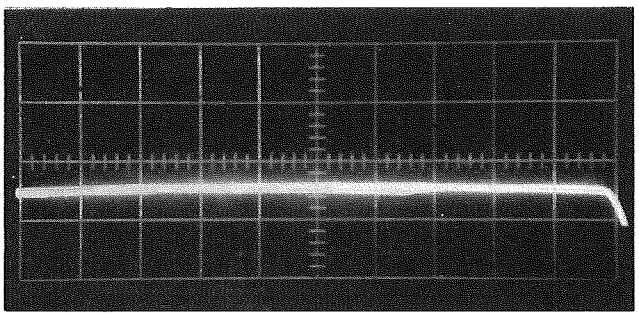

(b)

Fig. 11 - Effect of optical feedback
(a) no feedback (b) feedback from undeflected beam
Identical Scales

constant instead. Provided that the spurious orders are of low intensity (measurements summarised in Table 1 indicate that they contain less than 10% of the light present in the desired order at all input frequencies), this will hold the deflected beam constant as well. Results are as shown in Fig. 11. Fig. 11a shows the deflected beam intensity vs frequency over the full 80–140 MHz range of the system with no levelling; Fig. 11b shows the intensity with levelling. Unfortunately, the laser light had a substantial modulation at 100 Hz, due to ripple on its internal power supply, but the results suggest that the residual intensity variation is less than 10% of that encountered before levelling. This compares with the figure quoted for the intensity of spurious orders and would therefore appear to be the optimum obtainable from this technique. Suitable optics would enable spurious orders to be collected and sensed, in addition to the undeflected beam, and would possibly provide even better results.

Table 1

Driving Frequency (MHz)	Intensities of Orders of Refraction (mW) 1st Order	2nd Order	−1st Order	−2nd Order
83	>0·2	0·004	0·006	negligible
104	>0·2	0·004	0·030	..
138	0·016	negligible	0·006	..

Intensities of Spurious Order Radiation

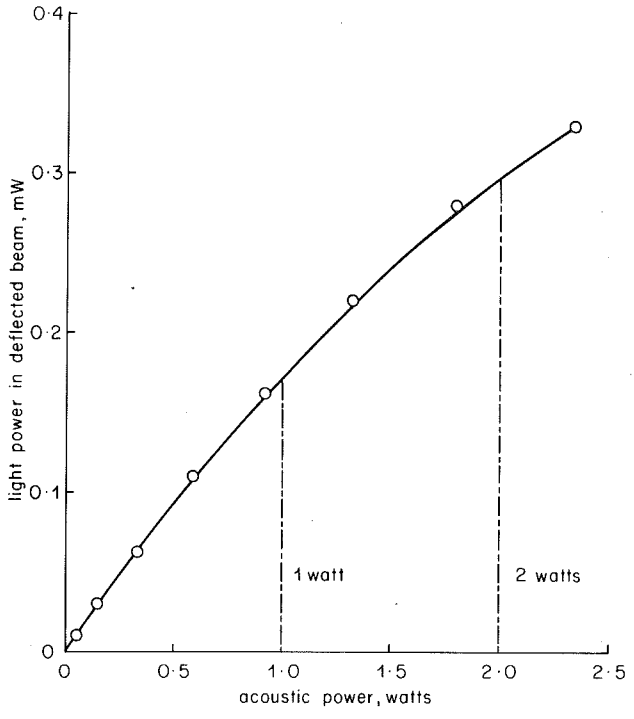

Fig. 12 - Light power in deflected beam vs acoustic signal power

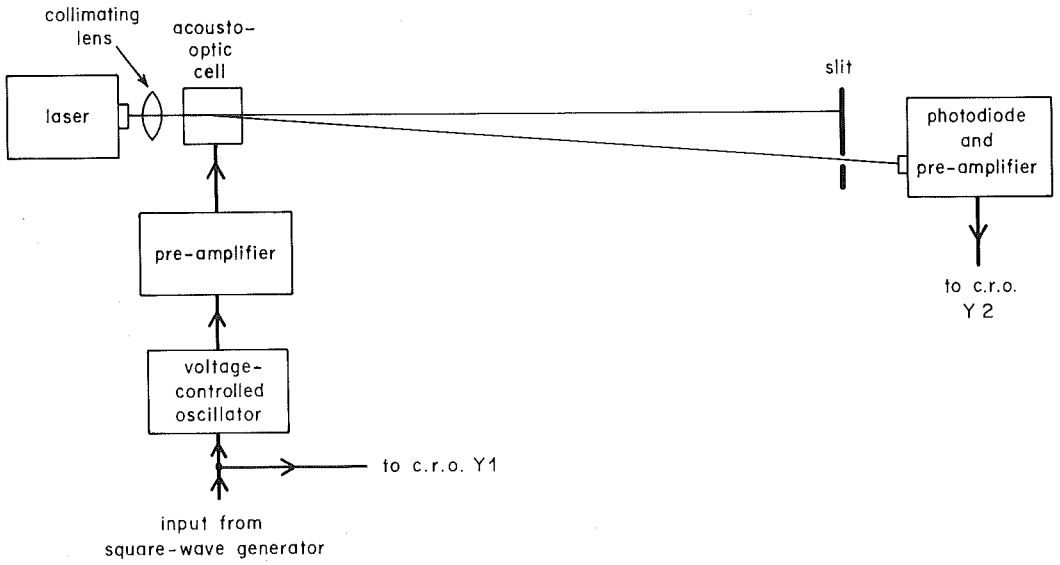

Fig. 13 - Arrangement for measuring time-domain response of cell

Fig. 12 shows the relationship between the intensity of the deflected spot and the amplitude of the acoustic input. The theoretical curve, drawn as a comparison, has the equation:

$$\text{Light Power} = 0{\cdot}48 \sin^2 AV \quad \text{(mW)} \qquad (7)$$

where V is the peak-to-peak electrical input in Volts and A is fixed by trial and error at 14°/V.

The experimental points are seen to be close to this line with a small systematic offset due probably to an inaccuracy in the measurement of the intensity in the laser output (measured at 0·48mW after passing through all the optics of the system, but with no acoustic input to the cell).

Another factor of interest is the time-domain response of the deflected cell to a sudden change in the acoustic frequency. To measure, this the system of Fig. 13 was set up. The input frequency to the cell was switched rapidly between two values and the slit was arranged to pass only the beam corresponding to one of these values. Overall results are shown in Fig. 14. The upper trace corresponds to the acoustic frequency while the lower trace is the measured intensity passing through the slit. It is seen that there is a delay of about 2·9 μsec before the change in acoustic frequency reaches the optical aperture and a further transit time of about 1·8 μsec as the change propagates across the optical aperture and the intensity of the beam builds up to its final value.

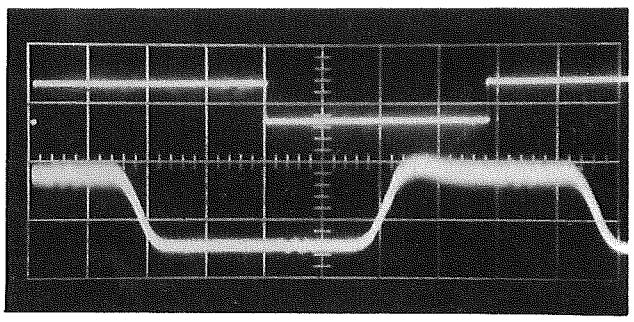

Fig. 14 - Time-domain response of cell
Horizontal Scale 2μsec/cm

(N.B. The polairty is chosen so that the light is switch from the position passing through the slit to the position that does not pass; as soon as the input frequency changes, the light corresponding to this frequency is interrupted by the edges of the slit. Thus a very accurate time reference is available, and any errors due to the square-wave not having a flat top are eliminated.)

Fig. 15 shows the spot profiles obtainable with the prototype system. The beam was scanned, at a slow rate (50 Hz) over the full 80—140 MHz acoustic range, and a slit was used to select a small fraction of this range for observation of the transmitted intensity. The number of resolvable spots obtainable with the prototype was 85·1, using a criterion that the spot width was equal to the distance between the peak and a point at which the amplitude had fallen to $1/e^2$ of its peak value. The spot profiles were then re-measured at a 20 kHz scan rate (Fig. 16). At this frequency the transit-time of the cell should cause a broadening of the spot profiles. The observed broadening was consistent with the hypothesis that the core of the beam occupies the central 70% of the available aperture.

Drift tests were carried out by measuring the acoustic frequency required for maximum transmittance through a fixed slit over a period of one hour. During this period

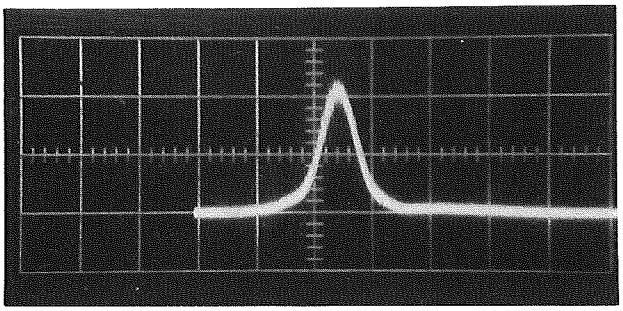

(a)

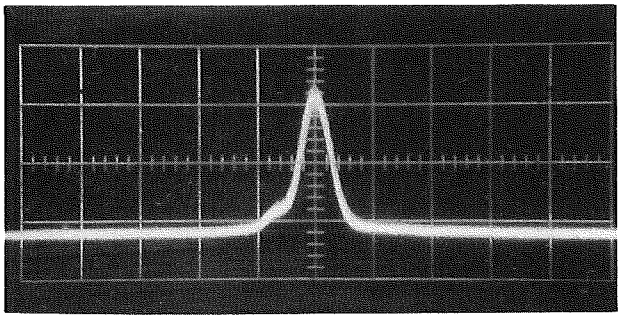

(b)

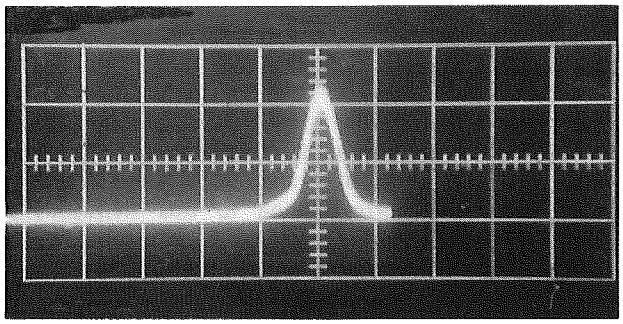

(c)

Fig. 15 - Spot profiles (50 kHz scan rate)
Horizontal Scale: 1cm = $\frac{1}{50}$ full scan

the frequency for maximum transmittance changed by a maximum of 100kHz, or about one sixth of a spot. Again, this is in line with the value of better than one quarter of a spot specified by the manufacturers.

The relative spectral transmittance was also measured and is shown in Fig. 17. It is seen that blue light (440 nm wavelength) does pass through the cell and therefore it is feasible to use the cell for a three-colour scanning application, such as telecine. Finally, the input reflection coefficient of the cell was measured, over the range 80–140 MHz. It can be seen from the results plotted on a Smith chart normalised to 50 Ohms (Fig. 18) that there is a considerable mismatch over the band. The effects of this have already been considered.

5. Conclusions and suggestion for improvement

A prototype laser deflection system has been constructed and evaluated; it has been shown to be feasible for the applications required. The use of feedback from the undeflected beam, to keep the intensity of the deflected beam constant, has been shown to produce a significant improvement. At higher scan speeds, however, the transit time of the cell becomes a major limitation on the

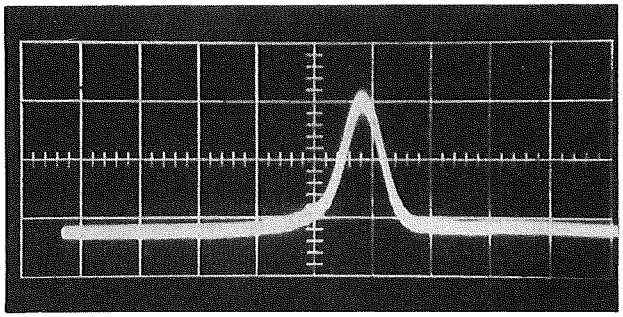

(a)

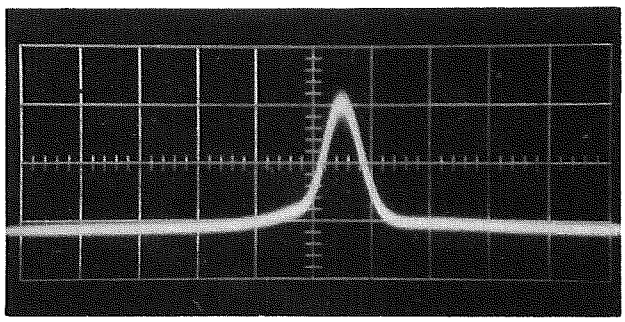

(b)

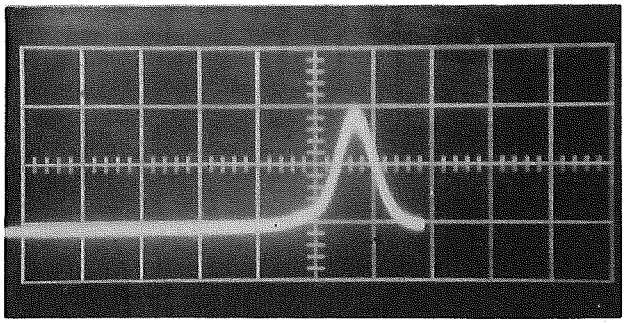

(c)

Fig. 16 - Spot profiles (20 kHz scan rate)
Horizontal Scale: 1cm = $\frac{1}{50}$ full scan

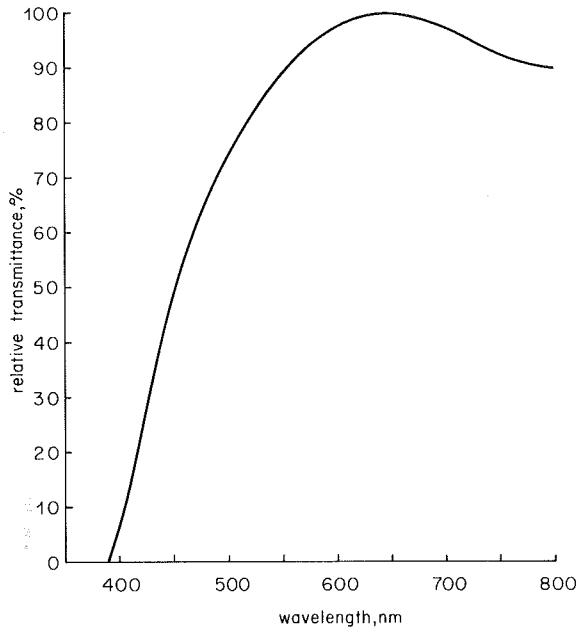

Fig. 17 - Spectral response of acousto-optic cell

effectiveness of this method and some refinements may be necessary, such as feedback from a previous scan, via a delay, to overcome this.

The spectral purity of the prototype system may not be sufficient for a telecine scanning application. This is because the frequency-control loop has been optimised for fast response. Decreasing the bandwidth of this loop would improve the spectral purity, at the expense of speed of response. For the holographic application, the speed of response is of prime importance, spectral purity being a secondary factor.

The optics of the prototype system left a lot to be desired. There is, therefore, scope for future work on more accurate measurement of parameters such as resolution, transit time, etc., and it is expected that such work will continue.

Part II

1. A comparison of the acoustic-optic method with other methods of laser deflection

Methods of light and laser deflection fall into five main categories. These will now be considered in more detail.

1.1 Variable reflection methods

Probably the earliest method of deflecting a light beam was the use of a rotating mirror or polygon of mirrors. Such a method, although providing a high resolution, (using the figures developed in Ref. 12 a resolution of 5000 spots at a 31 kHz scanning rate should be possible) is not very flexible, as it only allows a saw-tooth scan, whose rate cannot be changed very rapidly. Other methods involve mirrors mounted on a moving coil meter movement or on the end of a tuning fork.[13] Another method[14] uses a fibre optics bundle to convert a conical scan, obtained from a mirror mounted on the end of a thin quartz rod, to a linear scan. Finally a series of shear transducers has been used[15] to deflect a light beam by tilting a mirror over a small angle.

All the variable reflector methods have the advantage, when compared to the acoustic grating, that light of all colours is deflected by the same amount, making registration easy. They all suffer from the disadvantage that they rely on mechanical movement, however, which makes them restricted in bandwidth and not as versatile as the acoustic grating. In addition, all but the mirror design have a tendency to non-linearity especially if operated near resonance for reasonable efficiency.

1.2 Variable refraction methods

There are two basic approaches to the deflection of light by refraction. One consists of passing light through a prism, whose refractive index is varied by the electro-optic effect (e.g. Ref. 16). The other uses a refractive index gradient in a bar of electro-optic material to bend the beam.[17] This is analogous to the production of mirages by the bending of light by layers of air of different temperatures.

Another method uses acoustic waves to vary the refraction index of a material with the elasto-optic effect. This may be used to set up the refractive index gradient needed for deflection.[18] Note that the acoustic frequencies used for this are substantially lower than those used for the acoustic grating.

While the variable refraction methods are much more versatile than the variable reflection methods, they are dispersive; that is to say, light of different wavelengths is deflected by different angles. In addition most of these methods introduce a degree of optical distortion and are non-linear in terms of deflection vs the change in the quantity causing deflection.

1.3 Birefringent methods

Light passing through a birefringent material is deflected into two beams, containing light polarised in mutually perpendicular directions. If the incoming light is itself polarised in one of these directions, only one beam is transmitted. By switching the polarisation between one

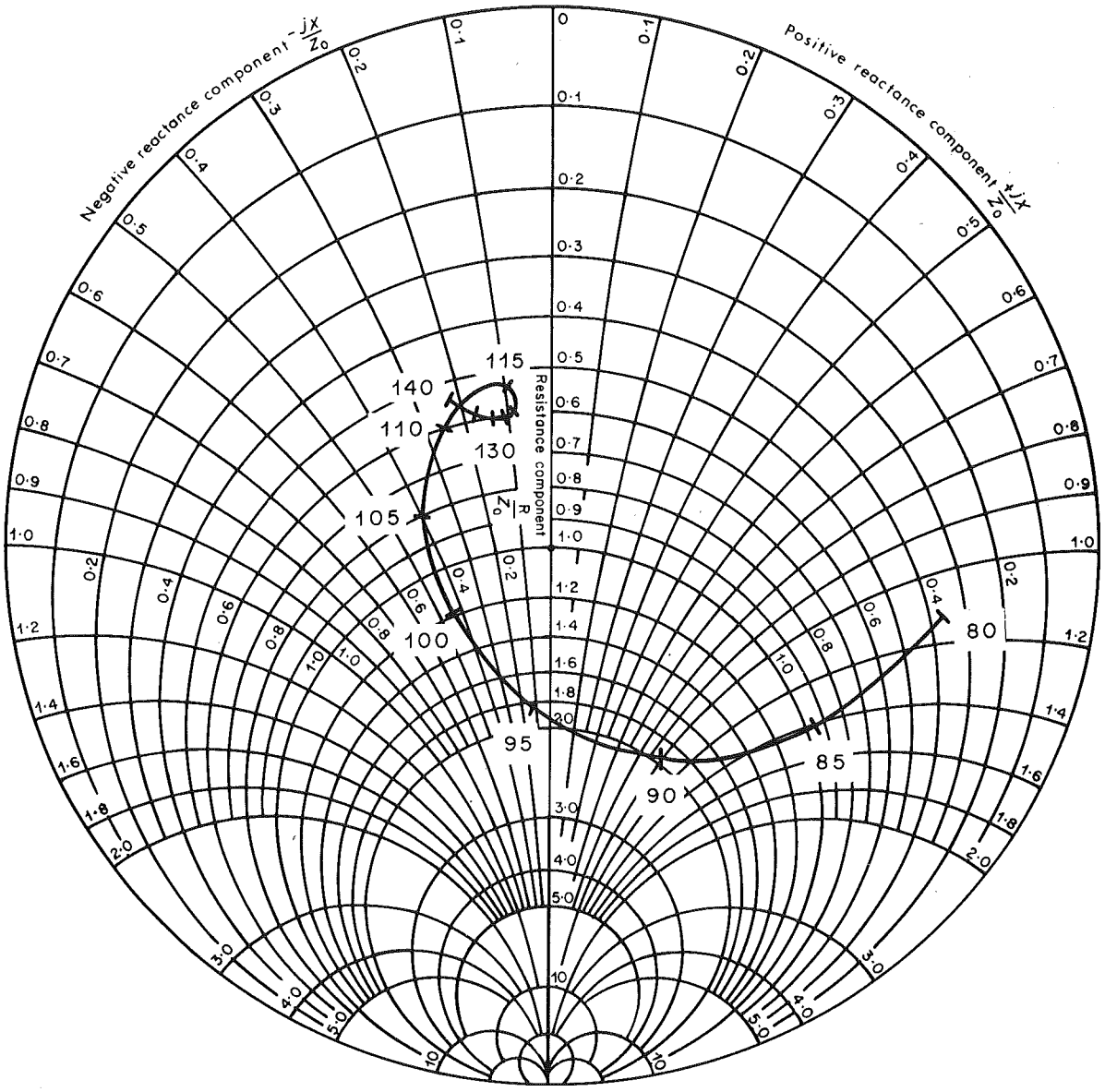

Fig. 18 - Input reflection coefficient of acousto-optic cell: spot frequencies shown in MHz

state and the other (by a Pockels cell or some similar appartus) the light can be switched from one beam to the other. If, then, the birefringent element is arranged in the form of a split-axis deflector[19] or a Wollaston prism[20] the two beams will be deflected by differing amounts according to the state of the polarisation.

This is a very powerful method of producing a deflection as it has a high potential resolution and linearity when stages are cascaded in a binary sequence. Unfortunately, both the birefringent element and the polarisation switch are wavelength-dependent and so the arrangement is essentially monochromatic. In addition the power dissipation in the polarisation modulator limits the speed to about 10^6 positions per second. Nevertheless, because of its inherently digital nature, it is probably the optimum method for holographic data retrieval, which only requires laser light of one wavelength.

1.4 Interference methods

Another method that has been used[22] is to produce a set of interference fringes by nearly parallel mirrors and to move them by varying the refractive index of the material between the mirrors. If one fringe is separated from the set, this can be scanned over a limited range. This method does, however, tend to give a low light efficiency. By far the most popular methods in this category are the acoustic grating and the electro-optic grating[21] which is similar in concept.

The resolution is limited, for any given scanning speed, by the transit-time-bandwidth product of the grating. Assuming a given maximum fractional-bandwidth, if the centre frequency can be raised into the GHz region with no drastic reduction in efficiency, the resolution may be substantially improved. In addition, although the device is wavelength sensitive, registration of several colours is relatively easy, by making them travel different path lengths after deflection;[23] the same cell may then be used for all the different coloured beams.

It appears that the acoustic grating, because of its linearity and modest power requirements, is probably the best deflection method for producing a sawtooth sweep; because of its lower resolution than the birefringent system, however, the latter is probably more suitable for a holographic application. If the resolution of the acoustic grating could be improved by the methods suggested above, then it would probably be preferable to the birefringent method because of the other advantages it holds, although the birefringent method does have the advantage that the scan geometry is independent of temperature.

1.5 Deflection methods internal to the laser

There have been some methods proposed for varying the 'angle of fire' of the laser directly. One of them[24] uses Kerr cells to switch the laser to one of several preferred directions. This method uses one Kerr cell per direction. Another method[25] uses a single Kerr cell to rotate the polarisation of the laser beam so that one direction, out of many, has most gain and will therefore lase most easily. This method is better, but requires that the laser be controlled so that it is on the verge of ceasing to operate. The more directions that are provided, the better it must be controlled. Another method[26] uses a layer of KDP on the face of a CRT, which normally cuts the laser off. When irradiated by an electrol beam however, a single spot is produced which will allow laser operation. By scanning the electron beam over the layer, the output of the laser can be made to follow.

Although these methods are interesting, they suffer from the disadvantage that they are necessarily single-wavelength devices. In addition, the resolution of the first two methods is severely limited.

2. Conclusions and suggestions for improvement

The results obtained in Part I indicate that the acousto-optic grating is potentially capable of fulfilling both of two applications, a digital holographic reader and a linear light scanner, although it may not be the best method for the first of these applications. However, the final system that could be used in the two cases would be very different. For the scanning application, the aperture of the device would be increased, to permit a higher resolution, and a cylindrical lens would be used to correct the defocussing caused by transit-time effects. Using the maximum possible aperture (that giving a transit time of 12 μsec) would enable 1000 spots per scan to be resolved, if the figures quoted in Part I can be reliably extrapolated. Some form of optical feedback from the undeflected beam would be necessary to keep the overall amplitude constant while, to reduce the drive power required and to reduce the light contained in spurious orders, the deflecting crystal would be made thicker, Bragg angle tracking methods then being used to increase the Bragg angle tolerance.

For the holographic application, a trade-off in design between spot-size and deflection-speed is apparent. There will probably be an optimum speed, when all other factors (such as complexity of light modulators and demodulators needed to produce and detect the digital pattern in the hologram) are taken into account. The laser deflector would therefore be designed to fulfil this requirement. Because the beam intensity is of secondary importance, feedback from the undeflected beam will probably be unnecessary (provided that the variation in light intensity is less than 10 – 20%).

Both applications will benefit from any development in materials, enabling higher acoustic frequencies to be used in the device; this would increase the resolution without increasing the transit time.

References

1. BORN, M *and* WOLF, E. 1959. Principles of Optics. London, Pergamon, 1959.

2. COHEN, M.G. *and* GORDON, E.I. 1965. Acoustic Beam Probing using optical techniques. *Bell Syst. Tech. J.*, 1965, **44**, 4, pp. 693–721.

3. BRILLOUIN, L. 1922. Diffusion de la lumiere et des rayons X par un corps transparent homogene. Ann. Phys. (France), 1922, 9th ser. **17**, p. 18. Also: 'La diffraction de la lumiere par les ultracons.' Paris, Hermann, 1933.

4. DEBYE, P. *and* SEARS, F.W. 1932. On the scattering of light by supersonic waves.' *Proc. Nat. Acad. Sci (USA)*, 1932, **18**, p. 409 (1932), also: LUCAS, R *and* BIGUARD, P. 1932. Optical properties of solids liquids under ultrasonic vibrations. *J. Phys.Rad.*, 1932, 7th ser. **3** p. 464.

5. GORDON, E. 1966. A review of acousto-optical deflection and modulation devices *Appl. Optics*, **5**, 10, pp. 1629–1639.

6. QUATE, C.F., WILKINSON, C.D.W. *and* WINSLOW, D.K. 1965. Interaction of light and microwave sound. *Proc. IEEE*, 1965, **53**, 10, pp. 1604–1623.

7. KORPEL, A. ADLER, R., DESMARES, P. *and* WATSON, W. 1966. A television display using acoustic deflection and modulation of coherent light. *Proc. IEEE*, 1966, **54**, 10, pp. 1429–1437.

8. GERIG, J.S. *and* MONTAGUE, H. 1964. A simple optical filter for chirp radar. *Proc. IEEE*, 1964. **52**, 12, p. 1753.

9. RCA RF Power Transistors Application Note AN3749.

10. JASIK, H. 1961. Antenna Engineering Handbook, New York, McGraw-Hill, 1961. Chapter 31.

11. ARNDT, F. 1967. High-Pass Transmission-Line Directional Coupler. *IEEE Trans Microwave Theory and Tech.*, 1968, **5**, pp. 310–311.

12. FOWLER, V.J. *and* SCHLAFER, J. 1966. A Survey of laser beam deflection techniques. *Proc. IEEE*, 1966, **54**, 10, pp. 1437–1444.

13. DOSTAL, F. 1966. The fork as a scanner: a new twist. *Electronic Communicator*, 1966, **1**, pp. 4–5.

14. ALSABROOK, G.M. 1966. A multicolour laser display. 18th Annual National Aerospace Electronics Conference, 1966. pp. 325–331.

15. SCHLAFER, J. *and* FOWLER, V.J. 1965. A precision, high speed, optical beam steerer. 1965. International Electron Devices Meeting.

16. CLEN, F.S. et.al. 1966. Light modulation and beam deflection with potassium tantalate-niobate crystals. *J.Appl. Phys*, 1966, **37**, pp. 388–398.

17. FOWLER, V.J. BUHRER, C.F. *and* BLOOM, L.R. Electro-optic light beam deflector. *Proc. IEEE*, 1964, **52**, 2, pp. 193–4.

18. GIAROLA, A.J. *and* BILLETER, T.R. 1963. Electro-acoustic deflection of a coherent light beam. *Proc. IEEE*, 1963. **51**, 8, pp. 1150–51.

19. NELSON, T.J. 1963. Digital Light Deflection *Bell Syst. Tech. J.*, 1964, **43**, 3, pp. 821–845.

20. SOREF, R.A. *and* MCMAHON, D.H. 1966. Optical design of Wollaston-prism digital light deflectors. *Appl. Optics*, 1966. **5**, p. 425 (1966).

21. COHEN, M.C. *and* GORDON, E.I., 1964. Electro-Optic (K. $Ta_xNb_{1-x}O_3$(KTN)) grating for light modulation and deflection. *Appl. Physics Lett.*, 1964, **5**, pp. 181–2.

22. KORPEL, A. 1965. Phased array type scanning of a laser beam. *Proc. IEEE*, 1965, **53**, pp. 1666–7.

23. WATSON, W.H. *and* KORPEL, A. 1970. Equalisation of acoustic-optic deflection cells in a laser colour t.v. system. *Appl. Optics*, 1970. **9**, 5, pp. 1176–9.

24. POLE, R.V., MYERS, R.A. and NUNEZ, J. 1965. Bi-directional electrically switched laser. *Appl. Optics*, 1965. **4**, pp. 119–121.

25. MYERS, R.A., POLES, R.V. *and* NUNEZ, J. 1965 Laser deflection with conjugate plane-concentric resonator. *Appl. Optics*, 1965, **4**, pp. 140–141.

26. MYERS, R.A. 1968. Fast electron beam scanlaser. *IEEE J. Quantum Electronics*, **QE-4**, 6, pp. 408–411.

APPENDIX I

Specification of prototype driving equipment

Frequency range:	80 – 140 MHz ①
Input voltage range:	0·6 V
Linearity of frequency/voltage transfer characteristic:	better than ± 135 kHz (0·225%)
Maximum rate of change of frequency:	4 μsec for 80 – 140 MHz sweep ② 1·4 μsec for flyback
Rise time to a small amplitude step input (to 90% of final value);	120 nsec
Drift:	less than 40 kHz after ½ hr warm-up
Output power into 50Ω:	> 1W
Output power into acoustic cell:	0·5 W approx.
Performance of power control loop (variations in power over a full 80 – 140 MHz sweep)	< ± 8% for scan speeds ⩽ 2 kHz < ± 12% for scan speeds ⩽ 16 kHz
Intensity variations of deflected beam using optical levelling	approx. ±5% at 1 msec scan speed ③
Level of spurious responses inside 80 – 140 MHz band:	–40 dB wrt main response
Spectral width of main oscillator output:	±30 kHz at –30 dB

Notes:

① Small-signal stages cover the range 35–160 MHz, but with reduced performance from the frequency control loop.

② The slew rate has been deliberately limited by the input buffer amplifier. The frequency control loop alone can slew at the rate of 210 MHz/μsec but if this rate is exceeded, the biaslevels in the oscillator are upset and may take several microseconds to restabilise. During this time the oscillator output is unpredictable.

③ The figure quoted is derived by synchronising the scan to the 50 Hz mains, thus eliminating to a large extent the ripple caused by the 100 Hz amplitude modulation of the laser.

APPENDIX II

Summary of measurements on acoustic cell

Mid-band deflection: (value calculated from velocity of acoustic wave in crystal =	18·2 m radian 18·5 m radian)
Deflection over frequency range 80 – 140 MHz: (theoretical value:	9·98 m radian 10·11 m radian)
Deflection efficiency at band centre 2½ W acoustic input): (manufacturer's specification:	71% > 70%)
Spot position accuracy (fraction of a spot): (manufacturer's specification:	$\frac{1}{6}$ better than ¼)
Transit time: (value calculated from velocity of acoustic wave over 7 mm aperture =	1·8 μsec 1·87 μsec)
Number of resolvable spots (50 Hz scan rate): (corresponding manufacturer's value,	85·1 80)
Number of resolvable spots (20 kHz scan rate): (Value assuming core of beam occupies 70% of aperture:	58·9 51·0)
Reflection coefficient of acoustic input	up to 72·5%

APPENDIX III

Description of driving circuits

The input buffer circuit is shown in Fig. 4a. It provides buffering and level shifting of the input signal so that it is of the correct amplitude and sign to drive the comparator. Two controls, R2 and R1 – a front panel set zero control – are used to set the d.c. level on the output.

The voltage-controlled oscillator is also shown in Fig. 4a and uses an integrated circuit oscillator controlled by a hyper-abrupt junction diode. This combination gives an output signal of greater than 600 mV peak to peak over the frequency range 35–150 MHz with a control voltage input of 1–12 V d.c. Two buffered outputs are provided.

One of these outputs feeds the pulse counting detector (Fig. 4a). Because of the high frequencies involved, the first stage of this detector divides the incoming frequency by a factor of 4. Tr5 and its associated components (Fig. 4a) perform the pulse counting operation, the output being a current proportional to the input frequency. The pulse rates involved are high and so the speed of response of this detector is good. The linearity, however, leaves something to be desired. For this reason a second detector, Tr3 and its associated components (Fig. 4a), is also provided operating at a slower speed. The slower speed, more linear, output is used to control the d.c. and low frequency components in the frequency control loop, whereas the high speed output controls the higher frequency components. This arrangement provides better linearity than is possible with the high speed detector alone, with a wider bandwidth than that available from the low-speed detector alone.

The comparator itself (Fig. 4a) is straightforward and serves merely to provide an amplified error voltage to drive the voltage controlled oscillator. The input filter was developed to give minimum phase shift in the range 0–4 MHz but greater than 26 dB attenuation at frequencies above 20 MHz (the pulse counting frequencies present in the detector). While the figure of 26 dB is adequate for the holographic application a higher figure would be needed for a flying-spot scanner. However, the bandwidth of the frequency-control loop would not need to be so great for the second application and so the filter design requirements are altered.

The preamplifier (Fig. 4b) is a conventional circuit, a.g.c. being applied to the first stage. From the preamplifier the signal passes to the main amplifier (Fig. 4b) which is a modified version of a 40W SSB power amplifier.[9] The two directional couplers DC1 and DC2 (Fig. 4b) provide a measure of the signal flowing to and reflected from the load. The outputs from these couplers are rectified and subtracted in the a.g.c. amplifier (Fig. 4b). Following on this operation, the signal is amplified and used to control the a.g.c. input of the preamplifier. A front panel control, R3 is used to set the output power level. If S1 (Fig. 4b) is switched 'on', a low-pass filter is introduced into the a.g.c. loop and any signals injected into the base of Tr14 are a.c. coupled into the feedback loop. This node is used to control the output power by an external photodetector looking at the undeflected beam.

Printed by BBC Research Department, Kingswood Warren, Tadworth, Surrey